

Supporting Information

Re-dispersion of Mo-based Catalysts and the Rational Design of Super

Small-sized Metallic Mo Species

Jiayi Chen¹, Haiyan Wang¹, Zhe Wang¹, Shanjun Mao¹, Jian Yu², Yong Wang² and Yong Wang^{1*}

¹Advanced Materials and Catalysis Group, Institute of Catalysis, Department of Chemistry, Zhejiang University, Hangzhou 310028, P. R. China.

²Center of Electron Microscopy and State Key Laboratory of Silicon Materials, School of Materials Science and Engineering, Zhejiang University, Hangzhou 310027, P. R. China.

*Corresponding author at: Advanced Materials and Catalysis Group, Institute of Catalysis, Zhejiang University, Hangzhou 310028, P. R. China.

E-mail address: chemwy@zju.edu.cn.

This PDF file includes:

Experiment section

Figure S1 to S15

Table S1 to S2

References

EXPERIMENTAL

Materials

Potassium hydroxide (KOH) and concentrated hydrochloric acid (HCl) were obtained from Sinopharm Chemical Reagent Co., Ltd. Sodium hydroxide (NaOH), sodium salicylate ($C_7H_5NaO_3$, AR, $\geq 99.5\%$), sodium nitroferricyanide dehydrate, sodium hypochlorite solution (5.0%) and dopamine hydrochloride were purchased from Aladdin. All chemicals without any further treatment were analytical. Commercial CC (carbon cloths, HCCP330) was purchased from Shanghai Hesen Electric Co. Ltd., China.

Electrochemical Measurements

Determination of ammonia

Spectrophotometry measurement with salicylic method¹: 6.404 g sodium salicylate and 1.28 g sodium hydroxide dissolved in 1000 mL deionized water which was used as coloring solution; A mixture of 8 mL sodium hypochlorite (5 wt %), 3 g sodium hydroxide and 100 mL deionized water was used as a oxidation reagent; 0.1g $Na_2[Fe(CN)_5NO] \cdot 2H_2O$ diluted to 10 ml with deionized water was used as catalyst reagent. Standard ammonium solution in the alkaline solution as follow: 4 mL of sample was taken. Then 50 μ L of oxidizing solution, 4 mL H_2O , 500 μ L of colouring solution and 50 μ L of catalyst solution were added respectively to the sample solution. Standard ammonium solution in the acid solution as follow: 4 mL of sample was taken. Then 4 mL H_2O , 1 mL KOH (1 M), 50 μ L of oxidizing solution, 500 μ L of colouring solution, 50 μ L of catalyst solution were added respectively to the sample solution. Absorbance

measurements were performed after 1 hour at $\lambda = 670$ nm. The calibration curve below was used to calculate the ammonia concentration.

Spectrophotometry measurement with Nessler reagent in the alkaline solution²:

NH₄Cl solutions with various concentrations were placed in the test tubes. Then KOH solution (0.1 M) were added to each test tube until the volume reached 10 mL. 1 mL sodium potassium tartrate (0.2 M) and 1 mL of Nessler reagent were added to each test tube one after another. Absorbance measurements were performed after 20 min at $\lambda = 425$ nm. The calibration curve below was used to calculate the ammonia concentration (Figure S13).

Determination of hydrazine

The hydrazine present in the electrolyte was estimated by the method of Di Bao and Qi Zhang.³ A mixture of 5.99 g para-(dimethylamino) benzaldehyde, 300 mL ethanol and 30 mL HCl (concentrated) was used as a color reagent. Calibration curve in the alkaline solution was plotted as follow: First, preparing a series of reference solutions and 3 mL of sample was taken; Second, adding 2 mL H₂O and 5 mL above prepared color reagent were added respectively to the sample solution, and then stirring 10 min at room temperature. Last, the absorbance of the resulting solution was measured at 456 nm. Calibration curve in the acid solution was plotted as follow: 2 mL of sample was taken. Then 2 mL H₂O, 1 mL KOH (1 M) and 5 mL color reagent were added respectively to the sample solution, and then stirring 10 min at room temperature. Last, the absorbance of the resulting solution was measured at 456 nm.

Faradaic efficiency

The Faradaic efficiency for NRR was defined as the quantity of electric charge used for synthesizing ammonia divided by the total charge passed through the electrodes during the electrolysis. The total amount of NH_3 produced was measured using colorimetric methods. Assuming three electrons were needed to produce one NH_3 molecule. The Faradaic efficiency could be calculated as follows: $\text{FE} = 3F \times [\text{NH}_3] / (17 \times Q)$, where F is the Faraday constant, $[\text{NH}_3]$ is the concentration and Q is total charge passed through the electrodes during the reaction duration according to the total current density. The rate of ammonia formation was calculated using the following equation: $R_{\text{NH}_3} = [\text{NH}_3] / t \times m$, where t is the reduction reaction time (h) and m is the loading mass of catalysts (mg cm^{-1}).

Computational Methods

All the theoretical calculations were performed using a plane-wave technique implemented in Vienna ab initio simulation package (VASP)^{4, 5} and the revised PBEsol functional.⁶ PBEsol functional was used as exchange-correlation functional approximation. The electron-ion interactions were expounded by the projector augmented wave (PAW) approach presented by Blöchl⁷ and carried out by Kresse⁸ and a plane-wave cutoff energy of 400 eV was used. A Monkhorst–Pack k-point mesh of $4 \times 4 \times 1$ and $2 \times 2 \times 1$ were used for the Brillouin zone sampling during electronic structure calculation and the structure optimization, respectively. The vacuum space along the z direction was set to be 15 Å and the periodic condition was employed along the x and

y directions. All atoms in the supercell are allowed to relax during the structure optimization except the bottom layer atoms of graphene. The relaxation was stopped when the force residue on the atom was smaller than 0.02 eV/Å. The adsorption energy for metal nanoparticles is defined as

$$E_{\text{ads}} = E_{\text{tot}} - E_{\text{slab}} - E_{\text{metal}}$$

where E_{tot} is the total energy of support and metal nanoparticle, E_{slab} is the energy of the clean support alone, and E_{metal} is the energy of metal nanoparticle.

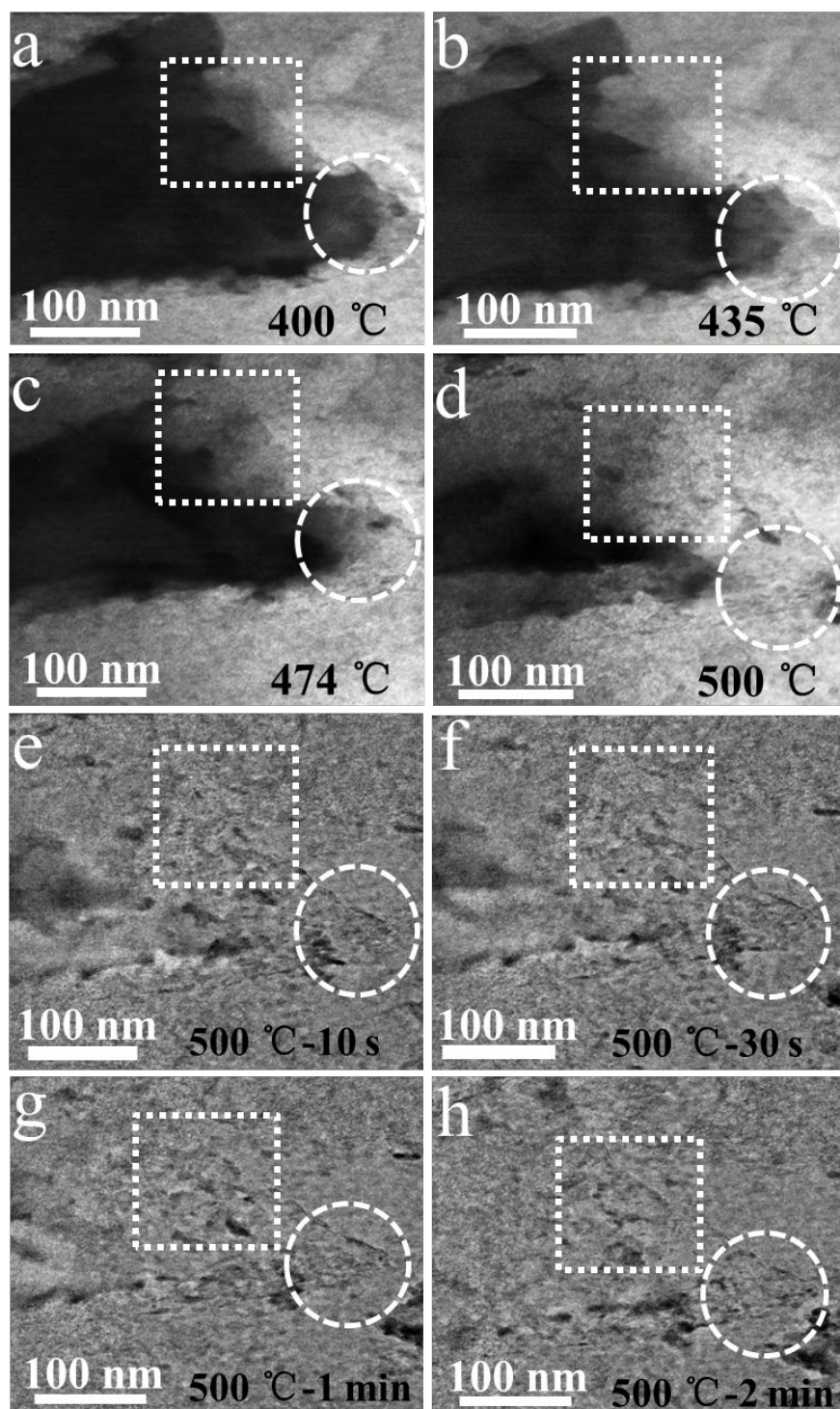


Figure S1 In-situ HRTEM images of the reduction of MoO₂/CC@CN in hydrogen starting 400 °C to 500 °C and then occurring at 500 °C for 5 min. (a) 400 °C, (b) 435 °C, (c) 474 °C, (d) 500 °C, (e) 500 °C for 10 s, (f) 500 °C for 30 s, (g) 500 °C for 1 min, (h) 500 °C for 2 min

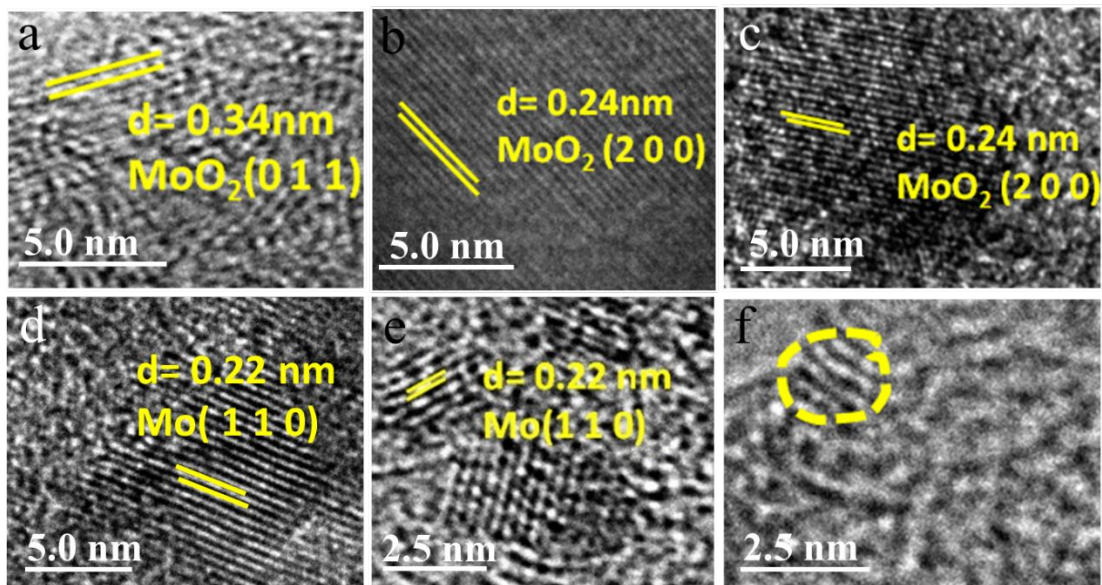


Figure S2 HRTEM images of (a) $\text{MoO}_2/\text{CC}@\text{CN}$, (b) $\text{MoO}_2\text{-}400\text{ }^\circ\text{C}\text{-}1\text{h}/\text{CC}@\text{CN}$, (c) $\text{MoO}_2\text{-}450\text{ }^\circ\text{C}\text{-}1\text{h}/\text{CC}@\text{CN}$, (d) $\text{Mo}\text{-}500\text{ }^\circ\text{C}\text{-}5\text{min}/\text{CC}@\text{CN}$, (e) $\text{Mo}\text{-}500\text{ }^\circ\text{C}\text{-}1\text{h}/\text{CC}@\text{CN}$ and (f) $\text{Mo}\text{-}500\text{ }^\circ\text{C}\text{-}8\text{h}/\text{CC}@\text{CN}$.

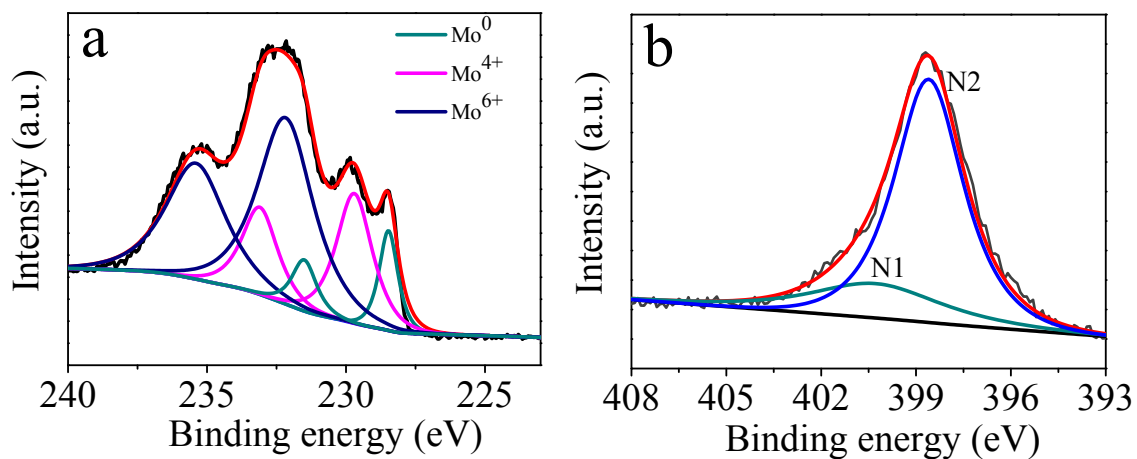


Figure S3 (a) and (b) The Mo 3d and N 1s XPS fine scan spectrum of $\text{Mo}\text{-}500\text{ }^\circ\text{C}\text{-}8\text{h}/\text{CC}@\text{CN}$ (N1: pyrrolic N, N2: pyridinic N), respectively.

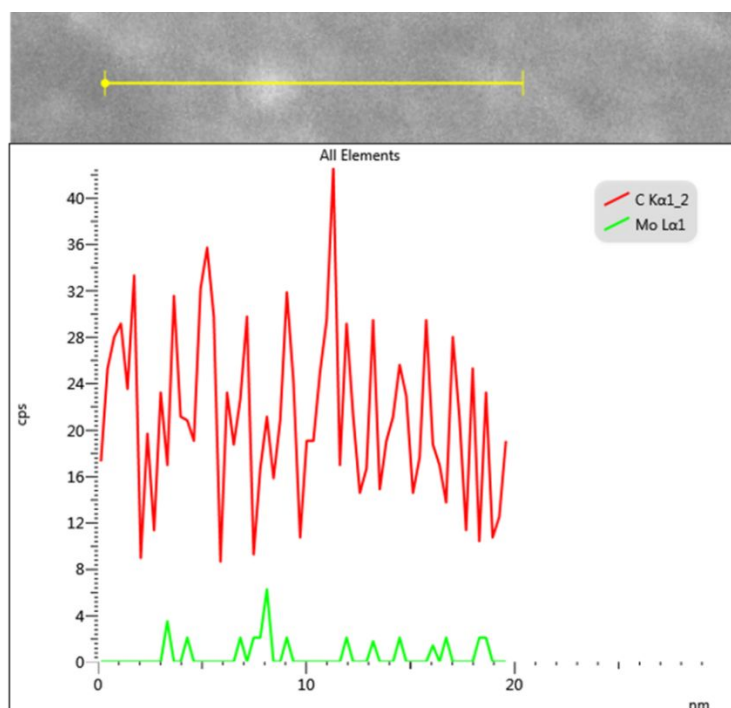


Figure S4 STEM-EELS line scan crossing a Mo-500 °C-10h/ACC-600.

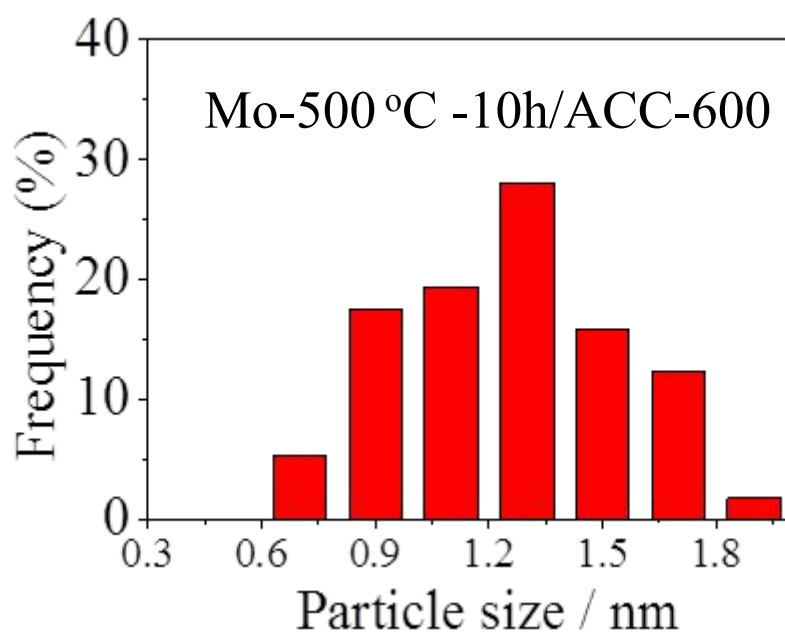


Figure S5 Mo nanoparticle size distribution of Mo-500 °C-10h/ACC-600.

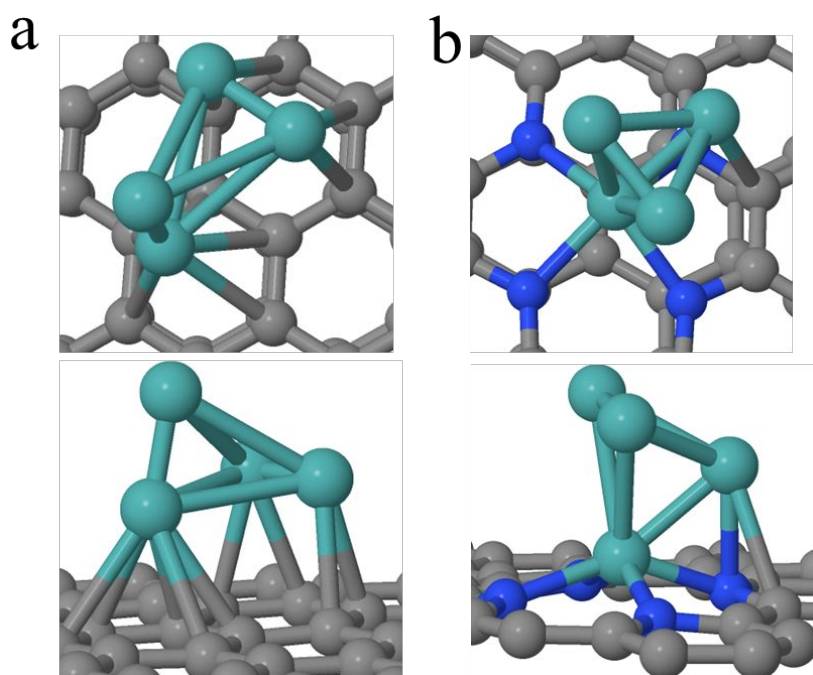


Figure S6 The top and side images of Mo-cluster on (a) graphene and (b) doped-N graphene (Mo: green; C: gray; N: blue)

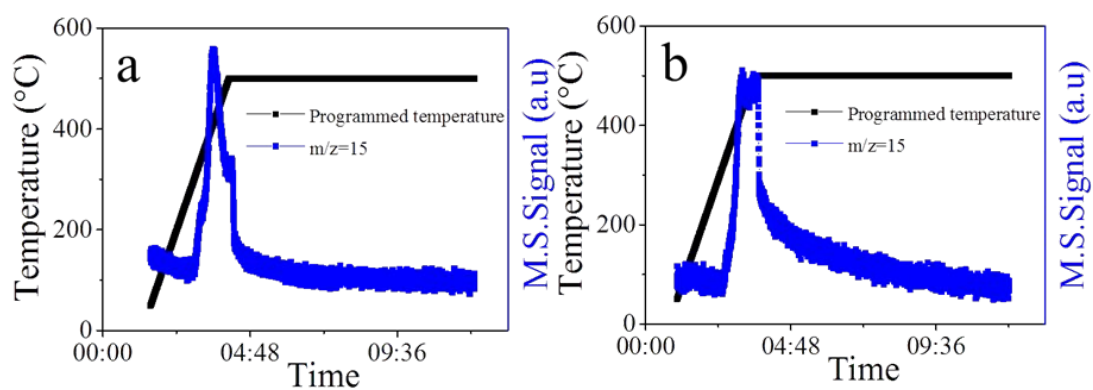
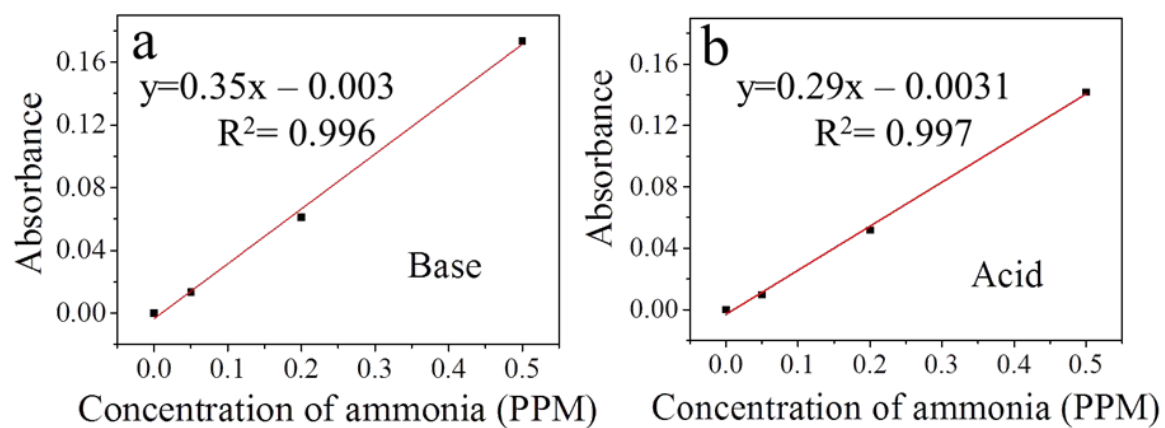
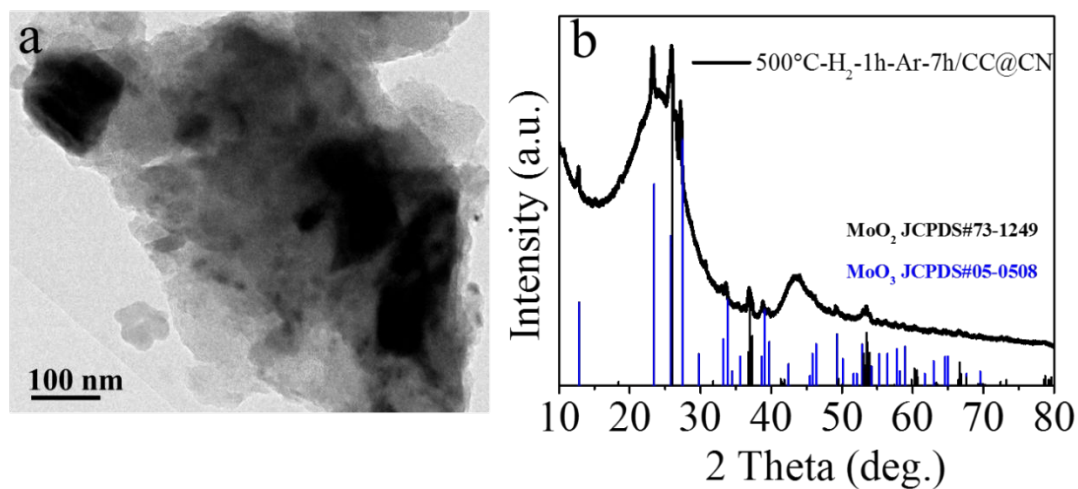


Figure S7 (a) and (b) H_2 -TPR-MS patterns of $\text{MoO}_2/\text{CC@CN}$ and $\text{MoO}_2/\text{ACC-600}$, respectively: mass spectra for CH_4 .



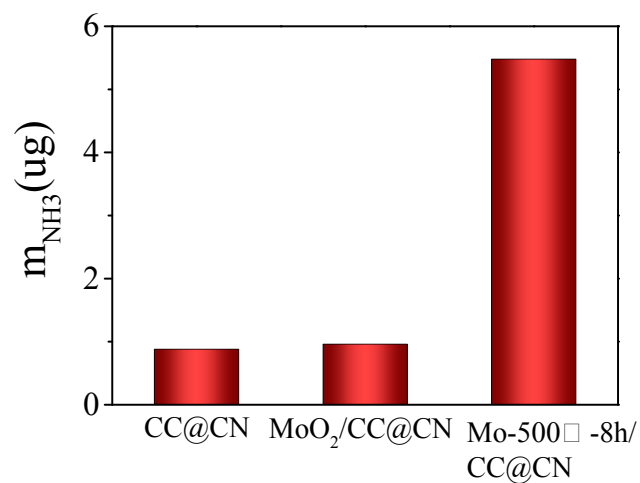


Figure S10 The amount of NH₃ with CC@CN, MoO₂/CC@CN and Mo-500 °C-8h/CC@CN electrode after 3h electrolysis at 0 V under ambient conditions, respectively.

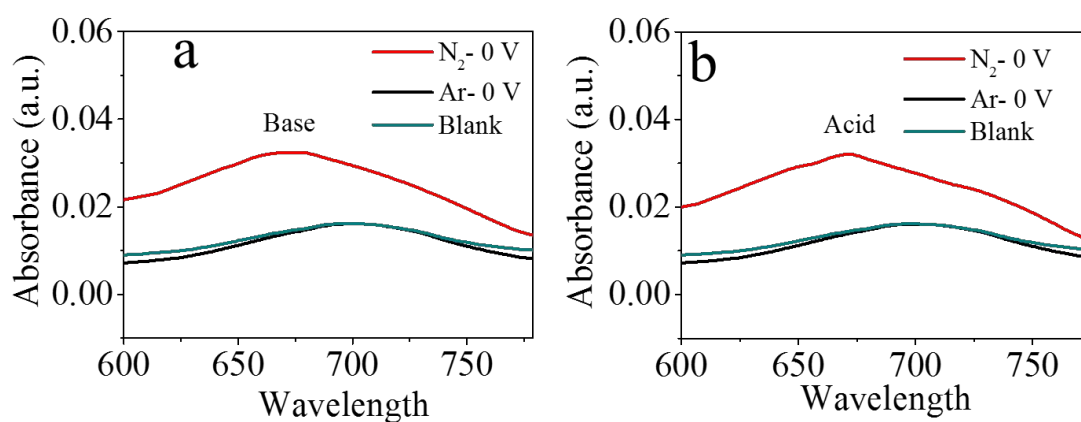


Figure S11 (a) and (b) UV-vis absorption spectra after potentiostatic tests in N₂ and Ar at 0 V versus RHE in base and acid, respectively.

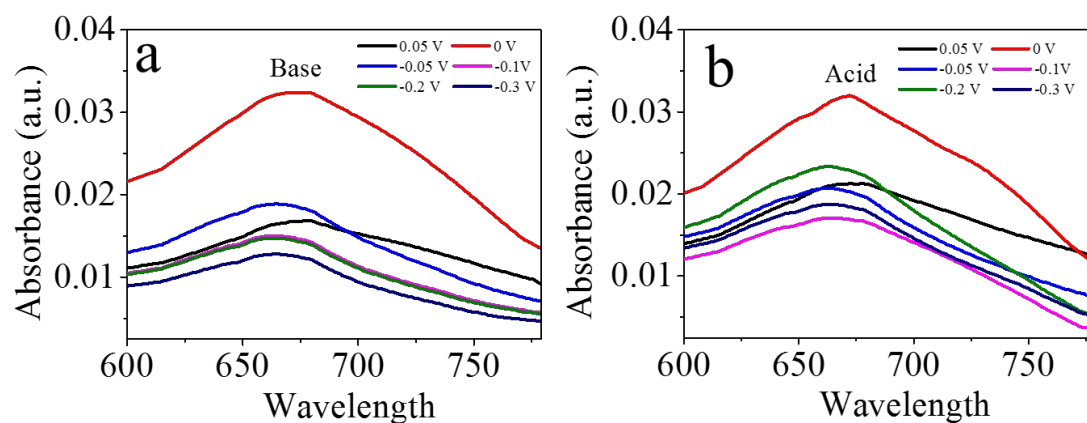


Figure S12 (a) and (b) Comparison of absorbance spectra at different potential in N_2 in base and acid, respectively.

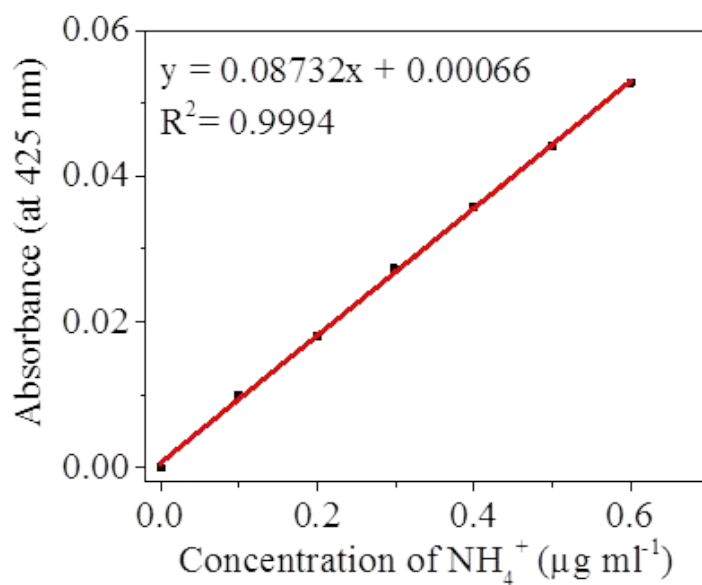


Figure S13 Calibration curve used for estimation of NH_3 in base using Nessler reagent.

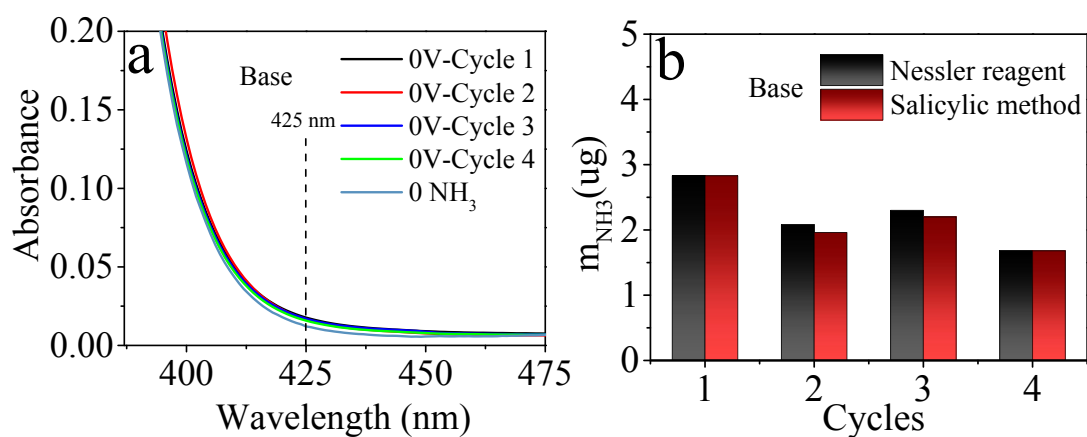


Figure S14 (a) Absorbance spectra of cycling test of Mo-500 °C-8h/CC@CN in base using Nessler reagent. (b) The amount of NH₃ with Mo-500 °C-8h/ CC@CN electrode after 3h electrolysis at 0 V under ambient conditions in base by Nessler reagent and Salicylic method, respectively.

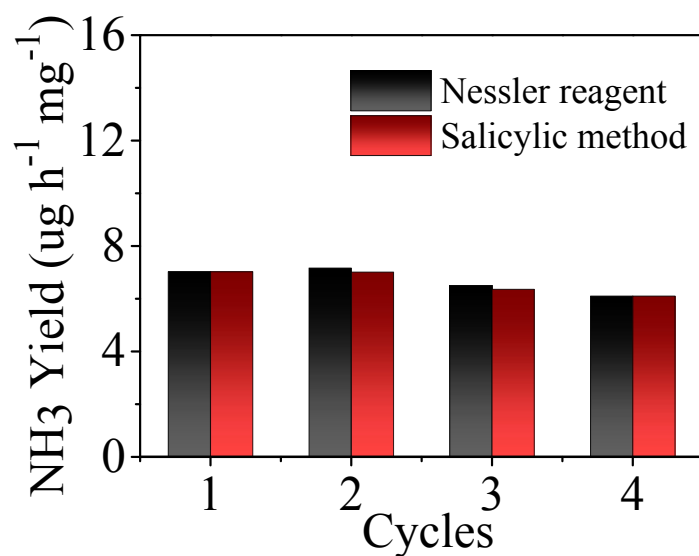


Figure S15 Yield of NH₃ with cycling test of Mo-500 °C-8h/CC@CN used by Nessler reagent and Salicylic method, respectively .

Table S1. The contents of Mo and N for Mo-500 °C-8h/CC@CN

Mo-500 °C-8h/CC@CN	Mo %	N %
Before calcination	1.35	0.27
After reduction	1.34	0.19

Table S2 Summary of the representative reports on N₂ fixation.

Process	System/Catalyst	Conditions	Yield	Testing Method	Reference
Harsh condition	Ru (7.8 wt%)-loaded Y ₅ Si ₃	400 °C	1.9 mmol g ⁻¹ h ⁻¹	Ion chromatography	Ref. 9
	Fe ₂ O ₃ /AC (Molten hydroxide)	250 °C, atmospheric pressure	8.27 × 10 ⁻⁹ mol s ⁻¹ cm ⁻²	Salicylic method	Ref. 10
	Fe/Ru-based catalysts	350~550 °C, 200~300 atm	~20% (N ₂ conversion rate)	----	Ref. 11
Electrocatalysis	Pt plate/0.1 M KOH/ N ₂ , Mo-500 °C -8h/CC@CN	room temperature and atmospheric pressure	7.03 ug h ⁻¹ mg ⁻¹ and 22.3% FE	Salicylic method	This work
	Pt plate/0.1 M HCl/ N ₂ , Au-TiO ₂ sub-nanocluster	room temperature and atmospheric pressure	8.11% (current efficiency)	Indophenol blue method	Ref. 12
	graphite plate/0.1 M KOH/ N ₂ , Au	room temperature and atmospheric pressure	1.648 ug h ⁻¹ cm ⁻² (NH ₃) 0.102 ug h ⁻¹ cm ⁻²	Nessler's reagent and Ammonia colorimetric assaykit	Ref. 3

			(N ₂ H ₄ H ₂ O)		
	Fe ₂ O ₃	250 °C, 25 bar, 1.0 V	35% (N ₂ conversion rate)	Salicylic method	Ref. 13
	Pt plate/ionic liquids, THF, ethanol/ N ₂ , Ni plate	room temperature	1.7% (current efficiency)	Berthelot method	Ref. 14
	Pt plate/0.1 M HCl/ N ₂ , amorphous- Au/CeO _x -RGO	room temperature and atmospheric pressure	8.3 ug h ⁻¹ mg ⁻¹ and 10.10% Faradaic efficiency (FE)	Indophenol blue method	Ref. 15
Photocatalysis	BiOBr, H ₂ O (sacrificial agent)	$\lambda > 420$ nm	1.08 ppm (1 h)	Nessler's reagent	Ref. 16
	Diamond, KI (sacrificial agent)	$\lambda > 190$ nm	0.8 ppm (24 h)	Indophenol blue method	Ref. 17

References:

1. Chen, S. M.; Perathoner, S.; Ampelli, C.; Mebrahtu, C.; Su, D. S.; Centi, G., Electrocatalytic Synthesis of Ammonia at Room Temperature and Atmospheric Pressure from Water and Nitrogen on a Carbon-Nanotube-Based Electrocatalyst. *Angew. Chem. Int. Ed.* **2017**, 56, 2699-2703.
2. Han, L.; Liu, X.; Chen, J.; Lin, R.; Liu, H.; Lu, F.; Bak, S.; Liang, Z.; Zhao, S.; Stavitski, E.; Luo, J.; Adzic, R. R.; Xin, H., Atomically Dispersed Mo Catalysts for High - Efficiency Ambient N₂ Fixation. *Angew. Chem. Int. Ed.* **2019**, 58, 2321-2325.
3. Bao, D.; Zhang, Q.; Meng, F. L.; Zhong, H. X.; Shi, M. M.; Zhang, Y.; Yan, J. M.; Jiang, Q.; Zhang, X. B., Electrochemical Reduction of N₂ under Ambient Conditions

for Artificial N₂ Fixation and Renewable Energy Storage Using N₂/NH₃ Cycle. *Adv. Mater.* **2017**, 29, 1604799.

4. Kresse, G.; Furthmuller, J., Efficiency of ab-initio Total Energy Calculations for Metals and Semiconductors using a Plane-wave Basis set. *Comp. Mater. Sci.* **1996**, 6, 15-50.

5. Kresse, G.; Furthmuller, J., Efficient Iterative Schemes for ab initio Total-energy Calculations Using a Plane-wave Basis set. *Phys. Rev. B* **1996**, 54, 11169-11186.

6. Hammer, B.; Hansen, L. B.; Norskov, J. K., Improved Adsorption Energetics Within Density-functional Theory Using Revised Perdew-Burke-Ernzerhof functionals. *Phys. Rev. B* **1999**, 59, 7413-7421.

7. Blochl, P. E., PROJECTOR AUGMENTED-WAVE METHOD. *Phys. Rev. B* **1994**, 50, 17953-17979.

8. Kresse, G.; Joubert, D., From Ultrasoft Pseudopotentials to the Projector Augmented-wave Method. *Phys. Rev. B* **1999**, 59, 1758-1775.

9. Lu, Y. F.; Li, J.; Tada, T.; Toda, Y.; Ueda, S.; Yokoyama, T.; Kitano, M.; Hosono, H., Water Durable Electride Y₅Si₃: Electronic Structure and Catalytic Activity for Ammonia Synthesis. *J. Am. Chem. Soc.* **2016**, 138, 3970-3973.

10. Cui, B. C.; Zhang, J. H.; Liu, S. Z.; Liu, X. J.; Xiang, W.; Liu, L. F.; Xin, H. Y.; Lefler, M. J.; Licht, S., Electrochemical Synthesis of Ammonia Directly from N₂ and Water over Iron-based Catalysts Supported on Activated Carbon. *Green Chem.* **2017**, 19, 298-304.

11. van der Ham, C. J. M.; Koper, M. T. M.; Hetterscheid, D. G. H., Challenges in

Reduction of Dinitrogen by Proton and Electron Transfer. *Chem. Soc. Rev.* **2014**, 43, 5183-5191.

12. Shi, M. M.; Bao, D.; Wulan, B. R.; Li, Y. H.; Zhang, Y. F.; Yan, J. M.; Jiang, Q., Au Sub-Nanoclusters on TiO₂ toward Highly Efficient and Selective Electrocatalyst for N₂ Conversion to NH₃ at Ambient Conditions. *Adv. Mater.* **2017**, 29, 1606550.

13. Licht, S.; Cui, B. C.; Wang, B. H.; Li, F. F.; Lau, J.; Liu, S. Z., AMMONIA SYNTHESIS Ammonia Synthesis by N₂ and Steam Electrolysis in Molten Hydroxide Suspensions of Nanoscale Fe₂O₃. *Science* **2014**, 345, 637-640.

14. Pappenfus T. M.; Lee K.; Thoma L. M.; Dukart C. R., Wind to Ammonia: Electrochemical Processes in Room Temperature Ionic Liquids. *ECS Trans.* **2009**, 16, 89-93.

15. Li, S. J.; Bao, D.; Shi, M. M.; Wulan, B. R.; Yan, J. M.; Jiang, Q., Amorphizing of Au Nanoparticles by CeO_x-RGO Hybrid Support towards Highly Efficient Electrocatalyst for N₂ Reduction under Ambient Conditions. *Adv. Mater.* **2017**, 29, 1700001.

16. Li, H.; Shang, J.; Ai, Z. H.; Zhang, L. Z., Efficient Visible Light Nitrogen Fixation with BiOBr Nanosheets of Oxygen Vacancies on the Exposed {001} Facets. *J. Am. Chem. Soc.* **2015**, 137, 6393-6399.

17. Zhu, D.; Zhang, L. H.; Ruther, R. E.; Hamers, R. J., Photo-illuminated Diamond as a Solid-state Source of Solvated Electrons in Water for Nitrogen Reduction. *Nature Mater.* **2013**, 12, 836-841.